

Interfacial Capacity between a Silver Bromide Solid Electrolyte and a Blocking Electrode

Noriyoshi KIMURA, Takahisa ŌSAKI, and Shinobu TOSHIMA

Department of Applied Chemistry, Faculty of Engineering, Tohoku University, Aramaki-Aoba, Sendai 980

(Received September 3, 1974)

The interfacial capacity between a silver bromide single crystal and graphite and platinum blocking electrodes was measured using an AC bridge in the potential range 0.05—0.55 V *vs.* Ag/AgBr at 200—400 °C. The observed capacity-potential curves were compared with the calculated values from the space charge layer capacity. In the case of the graphite electrode, the capacity had a minimum value at 0.15—0.20 V *vs.* Ag/AgBr, whereas for the platinum electrode, the capacity was considerably larger and the differential capacity-potential curves were complicated. It is concluded that the space charge layer capacity predominates for the graphite electrode, but for the platinum electrode, its interaction with silver ion must be taken into account.

The structure and polarization capacity of the interface between an electrode and an ionic crystal have been discussed by many researchers.¹⁻³⁾ In particular, the interfaces of ionic crystals containing excess electrons or positive holes as charge carriers, namely semiconductors, have been extensively investigated both theoretically and experimentally.^{4,5)} As is well known, in the neighborhood of a semiconductor surface, a space charge layer exists owing to charge excess or depletion, which is analogous to the Gouy-Chapman layer in an ionic aqueous solution.

In the case of an ionic conductive crystal, so called solid electrolyte, lattice defects act as charge carriers, and a space charge layer may be formed at the interface. Such a space charge layer model has been treated theoretically by Grimley and Mott,^{6,7)} and more recently by Kliewer.^{8,9)} The real crystal-electrode interface has been discussed many times and although considerable attention has been focussed on the measurements of the interfacial characteristics, we note that the measured values differ appreciably among researchers. This is probably mainly due to the uncertainty of the contact between crystal and solid electrode and partly due to the difficulty in preparing a clean and ordered surface of the crystals. These factors are particularly significant when polycrystalline samples are used.

In the present investigation, single crystals of silver bromide were used. A slight elasticity of the crystal enabled a good contact between the crystal and the electrode to be made. Since silver bromide has a simple crystal structure (NaCl type) and has Frenkel type lattice defects,¹⁰⁾ the interstitial silver ions and silver ion vacancies act as charge carriers in the crystal. Weiss¹¹⁾ measured polarization current when the electrode potential was changed, and then considered the space charge layer on the basis of the excess electron distribution in the silver bromide. Raleigh treated the interfacial capacity mainly by galvanostatic and potentiostatic charging method.¹²⁻¹⁴⁾ We measured the variations of the interfacial capacity with the electrode potential for both graphite and platinum as the blocking electrode in order to consider the interfacial characteristics.

Experimental

Sample Preparation. Silver bromide was prepared by adding hydrobromic acid to silver nitrate solution. All chemicals were of reagent grade and hydrobromic acid was distilled before use. The precipitate was dried under vacuum and melted in a quartz tube. After pinholing, the melted salt was treated in a bromine atmosphere and finally a pure sample was obtained by vacuum distillation. Single crystals were grown by the Bridgeman method. For the sample containing cadmium ion, a given amount of cadmium bromide was added to the silver bromide before vacuum drying. Then it was treated as described above except for the vacuum distillation. The crystal was machined into a disk 15 mm in diameter and 5 mm thick, and then polished. It was etched in 40% sodium thiosulfate and 0.2% potassium cyanide solution, and then washed well in redistilled water followed by heating in vacuum at about 200 °C. The sample preparation and cell assembly were carried out in the dark.

Cell Assembly. The working electrode was either a

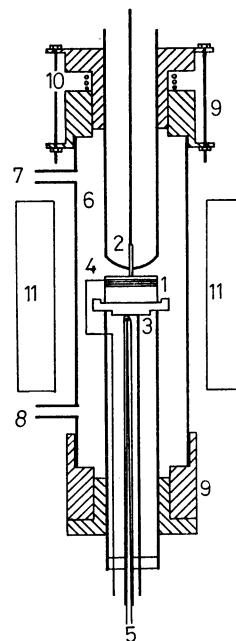


Fig. 1. Cell.

1: Solid electrolyte, 2: Working electrode, 3: Counter electrode, 4: Reference electrode, 5: Thermocouple, 6: Pyrex glass tube, 7: N₂ gas inlet, 8: N₂ gas outlet, 9: Brass holder, 10: Spring, 11: Electric furnace.

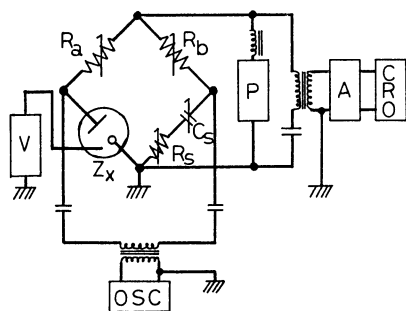


Fig. 2. AC bridge circuit.

P: Potentiometer, A: Tuning amplifier, CRO: Cathode ray oscilloscope, OSC: Oscillator, V: Electrometer.

wire of platinum or a rod of graphite, 1 mm in diameter. These electrodes were polished with γ -alumina (particle size 2μ), and were washed in acetone. The counter electrode was prepared by vacuum evaporation of silver on one plane of the cylindrical crystal pellet, and the silver foil was placed on it. For a reference electrode, silver wire was wound around the cylindrical pellet. The cell consisted of a silver bromide crystal pellet spring-loaded between the working and the counter electrodes as shown in Fig. 1. The cell was annealed in a nitrogen atmosphere at 400°C for half a day before measurement.

An AC bridge shown in Fig. 2 was used for impedance measurements. A potentiometer was included for applying a given potential to the working electrode. The input voltage to the bridge was regulated to be less than 5 mV p-p in the frequency range 0.2 to 10 kHz.

Results

Typical potential sweep curves were shown in Fig. 3. No appreciable rises in current were observed between 0.05 and 0.60 V. The current below 0.05 V is assumed to be due to deposition of silver and that beyond 0.60 V to be due to decomposition of silver bromide. So the differential capacity was measured in the range from 0.05 to 0.60 V. The observed capacity increases to some extent at low frequency, but it becomes almost constant at high frequency at higher temperatures. However, at temperatures below 250°C , the observed capacity decreases with increasing frequency above 1 kHz. In fact, the resistance of the crystal becomes

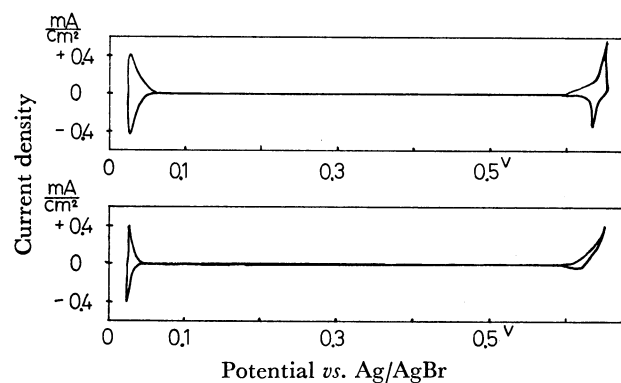


Fig. 3. Typical potential-current curve.

Upper: Pt/AgBr-CdBr₂ (0.5 mol%) at 350°C
Lower: Graphite/AgBr at 345°C
Potential sweep rate: 480 s/V

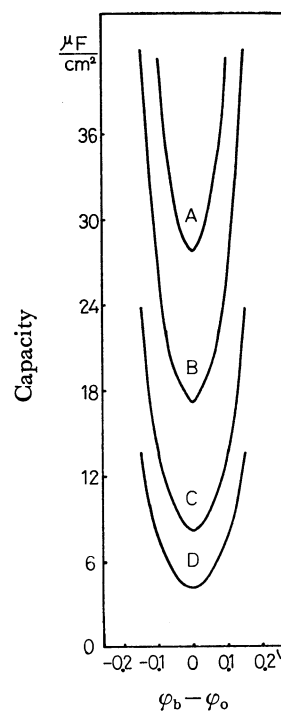


Fig. 4. The calculated value of space charge layer capacity for a silver bromide crystal.

A: 350°C , B: 300°C , C: 250°C D: 200°C .

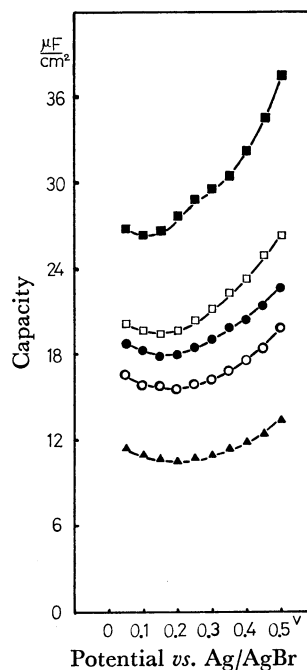
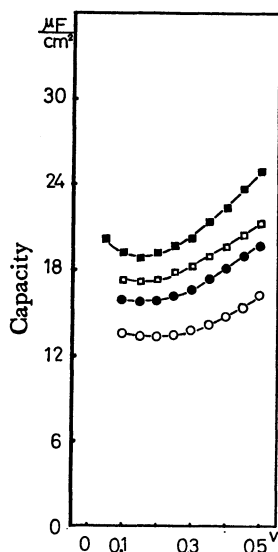


Fig. 5. Observed potential-capacity curves for graphite/AgBr.

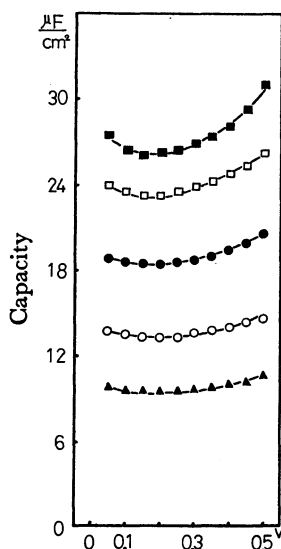
■: 395°C □: 350°C ●: 301°C ○: 248°C
▲: 219°C

considerable at this temperature, which suggests that the influence of the geometric capacity¹⁵⁾ seems to increase. Therefore, the capacity-potential curves were measured at a frequency of 1 kHz throughout this work.

The capacity-potential curves with graphite electrode are presented in Figs. 5—7 for silver bromide crystals which contained various amounts of cadmium bromide,

Potential vs. Ag/AgBr-CdBr₂ (0.1 mol%)Fig. 6. Observed potential-capacity curves for graphite/AgBr-CdBr₂ (0.1 mol%).

■: 402 °C □: 352 °C ○: 305 °C ●: 253 °C

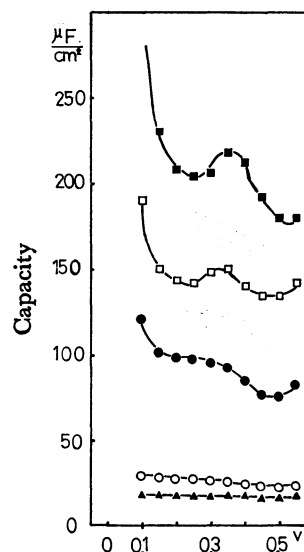
Potential vs. Ag/AgBr-CdBr₂ (0.5 mol%)Fig. 7. Observed potential-capacity curves for graphite/AgBr-CdBr₂ (0.5 mol%).

■: 397 °C □: 353 °C ●: 305 °C ○: 246 °C
▲: 209 °C

in order to change the amount of silver ion vacancies in them. The corresponding curves with a platinum electrode are shown in Figs. 8—10.

Discussion

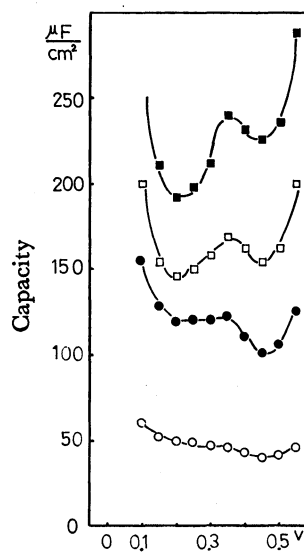
Space Charge Layer. Kliever⁹⁾ treated the space charge layer of silver chloride as a typical ionic crystal with Frenkel type defects. The same treatment may be applied to the silver bromide crystal. In a crystal slab of thickness $2L$, the potential φ will obey Poisson's equation with the boundary condition, $\varphi = \varphi_0$ at $x=0$, $x=2L$ (crystal surface) and $d\varphi/dx=0$, $\varphi = \varphi_b$ (in the



Potential vs. Ag/AgBr

Fig. 8. Observed potential-capacity curves for platinum/AgBr.

■: 399 °C □: 355 °C ●: 300 °C ○: 255 °C
▲: 200 °C

Potential vs. Ag/AgBr-CdBr₂ (0.1 mol%)Fig. 9. Observed potential-capacity curves for platinum/AgBr-CdBr₂ (0.1 mol%).

■: 400 °C □: 350 °C ●: 302 °C ○: 250 °C

bulk of crystal),

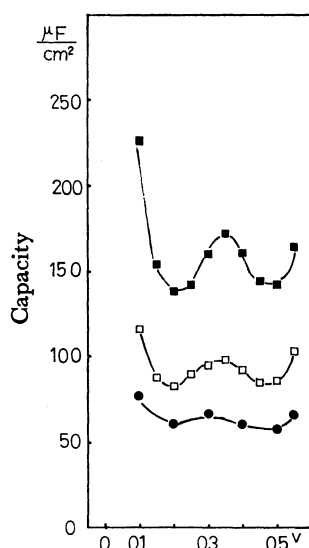
$$d^2\varphi/dx^2 = -4\pi\rho/\epsilon, \quad (1)$$

where ϵ is the static dielectric constant, ρ is the charge density in the crystal. In the silver bromide crystal, the densities of silver ion vacancy (effective charge: $-e$), n_v , and interstitial silver ion (effective charge: $+e$), n_i , are given by

$$n_v = N \exp \{[-F_v + e(\varphi - \varphi_0)]/kT\}, \quad (2)$$

$$n_i = N_i \exp \{[-F_i - e(\varphi - \varphi_0)]/kT\}. \quad (3)$$

assuming $n_v \ll N$, the density of silver ion lattice sites, and $n_i \ll N_i$, the density of interstitial sites, and the condition $2N = N_i$ is valid in the silver bromide crystal.



Potential vs. Ag/AgBr-CdBr₂ (0.5 mol%)

Fig. 10. Observed potential-capacity curves for platinum/AgBr-CdBr₂ (0.5 mol%).

■: 399 °C □: 350 °C ●: 303 °C

F_v and F_i are the formation free energy of the vacancy and the interstitial ion. If a divalent cation is introduced into the silver bromide, such a cation has an effective charge $+e$ when it does not associate with the vacancy. The density of unassociated divalent cations may be expressed as

$$n_t = N \exp \{[-\alpha - e(\varphi - \varphi_0)]/kT\}, \quad (4)$$

where α is a Lagrange multiplier. Thus, the charge density is given by

$$\rho = e(n_i - n_v + n_t). \quad (5)$$

Within the bulk of the crystal, the condition of electrical neutrality will be satisfied. The condition may be obeyed well when $\kappa L \gg 1$, where $1/\kappa = (\epsilon kT/8\pi e^2 N)^{1/2} \times \exp\{-(eU - F_v)/2kT\}$, substituting $U = \varphi_b - \varphi_0$. This value is about 1×10^{-7} cm, for the silver bromide crystal at 300 °C. For a pure crystal, the equation

$$U = (F_v - F_i + kT \ln 2)/2e \quad (6)$$

may be derived from the condition of electrical neutrality. Substituting Eqs. (2), (3), (4), and (5) into (1), and then integrating it, the electric field is found to be

$$d\varphi/dx = (32\pi kTN/\epsilon)^{1/2} \exp \{(eU - F_v)/2kT\} \times \sinh \{e(\varphi - \varphi_0)/2kT\}. \quad (7)$$

The surface charge density is given by $\sigma_0 = (\epsilon/4\pi) \times (d\varphi/dx)_{x=0}$. The space charge layer capacity is found to be $C_s = d\sigma_0/d\varphi_0$. In the bulk of the pure crystal, $n_{ib} = n_{vb} = n$ and $n = N \exp\{(eU - F_v)/kT\}$ are derived from the condition of electrical neutrality, so the capacity may be written

$$C_s = (\epsilon e^2 n / 2\pi kT)^{1/2} \cosh (eU/2kT). \quad (8)$$

Using Eq. (8), the capacity of the space charge layer for the silver bromide crystal was calculated and the result is shown in Fig. 4. This equation is similar to the space charge layer capacity for an intrinsic semiconductor.

Graphite Electrode. The differential capacity curves measured with the graphite electrode shown in Fig. 5 have a minimum value at a potential 0.15–0.20 V. With increasing temperature, the minimum point appears more sharply and the value of capacity increases, which is similar to the behavior shown in Fig. 4. The observed values of the capacity at minimum points agree fairly well with the calculated values of the space charge layer capacity. The crystals containing cadmium ion show similar characteristics to the pure crystal as shown in Figs. 6 and 7. This seems to be due to the fact that at high temperature intrinsic defects are predominant in the crystal lattice. A structure sensitive region for these crystals appeared in our conductivity-temperature measurements below 250 and 125 °C with crystals containing 0.5 and 0.1 mol% cadmium bromide, respectively. The observed capacity at these temperature varied little with potential in the neighborhood of the capacity minimum point, so that the potential of the capacity minimum was not remarkable.

The potential of zero charge on the silver bromide surface can be considered in connection with the potential of minimum capacity. If the formation energy of defects F_v and F_i were known, the potential of zero charge of the pure crystal can be calculated from the Eq. (6). Trautweiler¹⁶⁾ reported that the surface potential of the silver bromide was -0.14 V in reference to the crystal bulk. The potential of Ag/AgBr was reported to be 1.4 V by Mott and Grimley⁶⁾ and recently to be less than 0.6 V by Weiss.¹¹⁾ Then, the potential of zero charge on the silver bromide may be considered to be less than several hundred millivolts with reference to the potential of Ag/AgBr. In order to obtain a precise value of the zero charge potential in the solid-solid system, it may be difficult to employ the method of Karpachev,^{17,18)} who studied some fused metal electrodes on stabilized zirconia by potential-surface tension measurements. We would rather regard the observed potential of minimum capacity as the potential of zero charge in the case of the graphite electrode. Therefore, the differential capacity of the graphite in the measured potential range can be considered to be mainly due to the space charge layer capacity, caused by the distribution of the interstitial silver ions and silver ion vacancies.

Platinum Electrode. The observed capacity of the platinum electrode is considerably larger than that of the graphite electrode and the dependence on potential is complicated. The capacity curve had two minimum points at 0.20 and 0.45 V, and a small peak was observed between them. The shape of the differential capacity curve was not changed by addition of cadmium ion, therefore this characteristic was apparently not due to impurities. The same characteristic was observed by Raleigh¹²⁾ near the melting point. We consider it difficult to explain this capacity-potential relation by a simple space charge layer model, in which a charge carrier is regarded as an ideal point charge and its interaction with the electrode is not taken into account. In addition, the charge carriers in the real crystal have finite volume, therefore the closest distance of the ion

to the electrode and its interaction must inevitably be considered. This concept is similar to Stern's theory for ionic solutions, except for the solvent action. If an assumption is introduced that the ions interact with the electrode only in the layer adjacent to the surface (first layer), but the ions in the second and the following layer have a distribution determined by the space charge layer model, the electrode potential may be described as

$$\varphi_0 - \varphi_b = (\varphi_0 - \varphi_1) + (\varphi_1 - \varphi_2) + (\varphi_2 - \varphi_b), \quad (9)$$

where φ_1 , φ_2 , and φ_b represent the potential in the first and second layers and the bulk of the crystal. The surface charge density is given by

$$\sigma_0 = \sigma_1 + \sigma_s, \quad (10)$$

where σ_1 and σ_s denote the charge density in the first layer and the space charge layer. Then the capacity may be written as

$$\begin{aligned} 1/C &= \partial(\varphi_0 - \varphi_b)/\partial\sigma_0 \\ &= 1/C_{0-1} + (1/C_{1-2} + 1/C_s)(1 - \partial\sigma_1/\partial\sigma_0), \end{aligned} \quad (11)$$

where $C_{0-1} = \partial\sigma_0/\partial(\varphi_0 - \varphi_1)$, $C_{1-2} = \partial\sigma_s/\partial(\varphi_1 - \varphi_2)$, and $C_s = \partial\sigma_s/\partial(\varphi_2 - \varphi_b)$. C_s can be determined from Eq. (8), but if any interaction between ion and electrode is present, the observed capacity is not given by the simple space charge layer model. Thus, the platinum electrode is considered to show significant interaction with the silver ion. When there is no interaction, $\partial\sigma_1/\partial\sigma_0 = 0$, and therefore $1/C = 1/C_1 + 1/C_s$ is valid, where C_1 is the capacity which arises from the finite size of ions. The graphite electrode is considered to

have little interaction with the silver ion. When $C_1 \gg C_s$, the observed capacity is predominantly due to C_s .

This research was partly supported by the Science Research Fund of the Ministry of Education.

References

- 1) J. R. Macdonald, *Phys. Rev.*, **92**, 4 (1953).
- 2) H. Chang and G. Jaffe, *J. Chem. Phys.*, **20**, 1071 (1952).
- 3) R. J. Friauf, *ibid.*, **22**, 1329 (1954).
- 4) C. G. B. Garrett and W. H. Brattain, *Phys. Rev.*, **99**, 376 (1955).
- 5) H. J. Engell and K. Bohnenkamp, "The Surface Chemistry of Metals and Semiconductors", ed. by H. C. Gatos, John Wiley & Sons, New York (1960).
- 6) T. B. Grimley and N. F. Mott, *Disc. Faraday Soc.*, **1**, 3 (1947).
- 7) T. B. Grimley, *Proc. Roy. Soc. (London)*, **A201**, 40 (1950).
- 8) K. L. Kliever and J. S. Koehler, *Phys. Rev.*, **140**, A1226 (1965).
- 9) K. L. Kliever, *J. Phys. Chem. Solids*, **27**, 705 (1966).
- 10) J. Teltow, *Ann. Phys.*, **5**, 63, 71 (1949).
- 11) K. Weiss, *Ber. Bunsenges. Phys. Chem.*, **76**, 379 (1972).
- 12) D. O. Raleigh and H. R. Crowe, *J. Electrochem. Soc.*, **118**, 79 (1971).
- 13) D. O. Raleigh, *J. Phys. Chem.*, **70**, 689 (1966).
- 14) D. O. Raleigh, *ibid.*, **71**, 1785 (1967).
- 15) R. D. Armstrong and R. Mason, *J. Electroanal. Chem.*, **41**, 231 (1973).
- 16) F. Trautweiler, *Phot. Sci. Eng.*, **12**, 98 (1968).
- 17) A. T. Filyaev, I. D. Remez, and S. V. Karpachev, *Soviet Electrochem.*, **8**, 251 (1972).
- 18) S. V. Karpachov, V. V. Salnikov, and A. T. Filjayev, *Electrochem. Acta*, **18**, 319 (1973).